Journal of Medicinal Chemistry

Brief Article

pubs.acs.org/jmc

Assessing the Target Differentiation Potential of Imidazole-Based Protein Kinase Inhibitors

Dilyana Dimova,[†,∥] Preeti Iyer,[†,∥] Martin Vogt,[†] Frank Totzke,[§] Michael H. G. Kubbutat,[§] Christoph Schächtele,[§] Stefan Laufer,*[,‡] and Jürgen Bajorath*[,†]

[†]Department of Life Science Informatics, B-IT, LIMES Program Unit Chemical Biology and Medicinal Chemistry, Rheinische Friedrich-Wilhelms-Universität, Dahlmannstrasse 2, D-53113 Bonn, Germany

[‡]Department of Pharmacy and Biochemistry, Pharmaceutical/Medicinal Chemistry, Eberhard-Karls-Universität Tübingen, Auf der Morgenstelle 8, D-72076 Tübingen, Germany

[§]ProQinase GmbH, Breisacher Strasse 117, D-79106 Freiburg, Germany

Supporting Information

ABSTRACT: A library of 484 imidazole-based candidate inhibitors was tested against 24 protein kinases. The resulting activity data have been systematically analyzed to search for compounds that effectively differentiate between kinases. Six imidazole derivatives with high kinase differentiation potential were identified. Nearest neighbor analysis revealed the presence of close analogues with varying differentiation potential. Small structural modifications of active compounds were found to shift their inhibitory profiles toward kinases with different functions.

INTRODUCTION

Profiling of compound collections against target families is an important source of activity data for chemical biology and drug discovery.[1] Profiling has become a popular approach to characterize ligand-based relationships between targets[2] and identify new active compounds, especially for high-profile therapeutic targets such as G protein coupled receptors[3,4] or protein kinases.[5,6] Target profiling experiments are frequently carried out in pharmaceutical research environments, but these proprietary results are rarely disclosed, with occasional exceptions.[7,8] Exemplary profiling studies have substantially advanced our understanding of structure−activity relationships (SARs) and selectivity patterns within important target families. For example, profiling of kinase inhibitors against different subfamilies of the kinome revealed unexpected cross-reactivity of many kinase inhibitors,[7] hence providing insights into polypharmacological behavior of clinically relevant inhibitors. In addition, molecular network analysis has been applied to analyze kinase profiling data and rationalize activity patterns.[8] On the basis of kinase profiling data,[8] matched molecular pair analysis has also been carried out to propose inhibitors with increased kinase selectivity.[9] However, kinase profiling is a laborious and expensive part of medicinal chemistry programs, as it requires large assay efforts and high costs. Consequently, in silico support or guidance in study design and data analysis, even if approximate, should be of considerable help for the community. Several computational studies have analyzed available kinase activity data. For example, machine learning models have been derived to search for kinase inhibitors on a large scale[10] or process profiling data and predict cross-reactivity of kinase inhibitors.[11]

Herein, we report a kinase profiling experiment using a library of imidazole-based adenosine triphosphate (ATP) site-directed kinase inhibitors. Different from previous investigations, much emphasis has been put on the exploration of kinase differentiation potential of candidate inhibitors. The concept of kinase differentiation potential is distinct from kinase selectivity of inhibitors. Compounds with differentiation potential must display significantly varying potency levels against multiple kinases.

METHODS AND MATERIALS

Kinases, Inhibitors, and Profiling Assays. A set of 484 pyridinylimidazole based inhibitors with general structure **I** (Scheme 1) were tested for kinase inhibition using 24 different kinases (AKT1, ARK5, Aurora-A, Aurora-B, BRAF VE, CDK2/CycA, CDK4/CycD1, COT, AXL, EGF-R, EPHB4, ERBB2, FAK, IGF1-R, SRC, VEGF-R2, CK2-α1, JNK3, MET, p38-α, PDGFR-β, PLK1, SAK, TIE2). These kinases were selected because they are implicated in different forms of cancer. The 484 different derivates were synthesized and characterized (including their purity) as described previously.[12−17] Kinase activity data were generated with the ProQinase free choice biochemical kinase assay system. Activities were determined as residual activities (% of control).[18]

Scheme 1

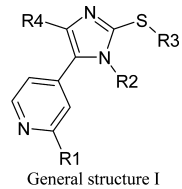

General structure I

Initially, compounds were screened at a single concentration of 10 μM. Subsequently, titration curves were generated for clearly active compounds. Then the coefficient of variation (CV) between the initial

Received: October 6, 2012
Published: December 4, 2012

dx.doi.org/10.1021/jm3014508 | J. Med. Chem. 2012, 55, 11067−11071

screen and subsequent assays was determined for each kinase. The average CV was only 7.7% (for only 3 of 24 kinases, values of 10−12% were obtained), thus indicating that activity data for the initial single-point experiments were reliable.

Analysis of Kinase Differentiation Potential. Residual activities for single-point measurements were logarithmically transformed into a numerically stable data format for subsequent analysis, as illustrated in Figure 1. According to this transformation, a logarithmic value of 2

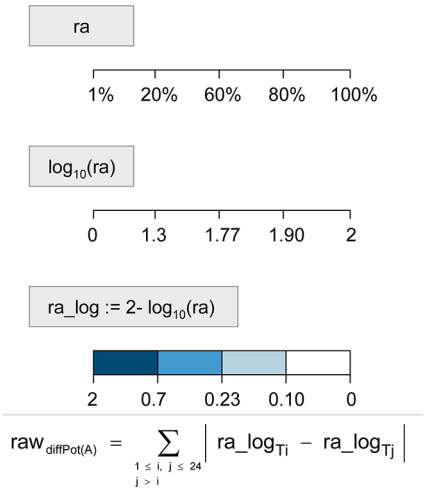

Figure 1. Scoring scheme. Measured residual activities (ra) were initially converted into logarithmic values used for the calculation of the raw differential potential ($raw_{diffPot}$) of each compound. Logarithmic values were adjusted such that 2 indicated (nearly) complete inhibition and 0 no inhibition and aligned with the original experimental binning scheme. Color code is as follows: dark blue, ≤20%; blue, >20%, ≤60%; light blue, >60%, ≤80%; white >80% residual wild-type activity.

indicates (nearly) full inhibition and a value of 0 no inhibition. On the basis of these transformed activity values, a raw target differentiation potential score was calculated as follows (see also Figure 1):

$$raw_{diffPot(A)} = \sum_{\substack{1 \le i,j \le 24 \\ j>i}} |ra\ log\ T_i - ra\ log\ T_j|$$

Here, the logarithmic terms refer to the transformed activity of a compound to targets T_i and T_j, respectively. For each compound, all possible target pairs were formed and activity differences were summed. Thus, according to this formalism, compounds have high differentiation potential if they display large activity differences against many target pairs. Raw scores were then transformed into standard *Z*-scores and normalized through mapping onto a cumulative distribution function assuming a normal distribution, yielding final scores between 0 (lowest differentiation potential) and 1 (highest potential). This scoring scheme represents a further refined and generalized version of a binned cumulative differentiation score previously used to characterize ligands of different target families.[19]

Nearest Neighbor Analysis. For selected active compounds, nearest structural neighbors were identified on the basis of systematic pairwise comparisons. For this purpose, Tanimoto similarity[20] was calculated using MACCS structural keys[21] as a molecular representation. As a nearest neighbor criterion, a threshold value of more than 80% MACCS Tanimoto similarity was applied.

Activity Profiles. For preferred inhibitors and their nearest neighbors, activity profiles were generated using the activity-based color code shown in Figure 1. In these profiles, each bin corresponds to the activity against a specific kinase.

RESULTS AND DISCUSSION

Kinase Inhibitor Data. The complete matrix reporting activities for all 484 compounds against the 24 kinases is provided in Table S1 of the Supporting Information. All residual activities were transformed into a logarithmic format (as described above) and subjected to computational analysis.

Compound Differentiation Potential. Figure 2 shows the distribution of normalized *Z*-scores for all test compounds.

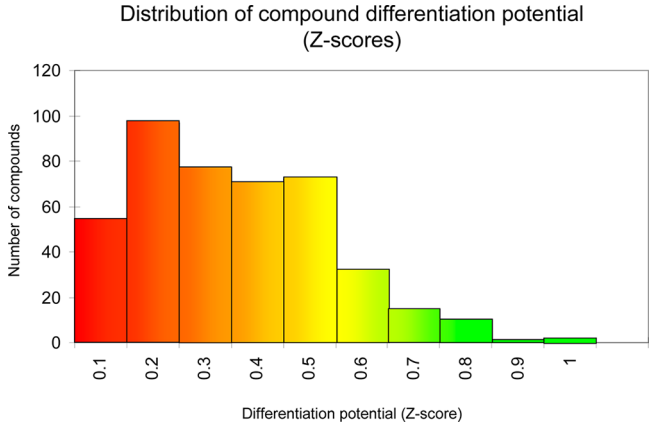

Figure 2. Distribution of compound differentiation potential. The histogram shows the distribution of *Z*-scores for all test compounds. *Z*-scores were normalized to the value range between 0 (lowest differentiation potential) and 1 (highest potential) and binned on the *X*-axis into 10 equally sized score intervals. The *Y*-axis reports the number of compounds falling into each interval. The differentiation potential of the compounds (normalized *Z*-scores) was color-coded using a spectrum ranging from red (lowest differentiation potential) over yellow (intermediate) to green (highest differentiation potential).

The score distribution directly reflects the kinase differentiation potential of the inhibitors. The distribution reveals that most of the compounds fell within the range of low (red) to intermediate (yellow) differentiation potential, as one might expect for ATP site-directed inhibitors. However, the distribution also contained a notable tail toward high (green) differentiation potential. Hence, a small subset of test compounds displayed a much higher than average potential to differentiate between the selected cancer-relevant kinases.

Preferred Inhibitors. On the basis of the score distribution in Figure 2, we selected the imidazole derivatives with the highest differentiation potential, falling into the scoring interval [0.78, 1.00]. The structures of these in part closely related analogues are shown in Figure 3 with their activity profiles.

In the next step, nearest structural neighbors of each of the six top-scoring compounds were identified in the data set and their differentiation potential was compared, as reported in Figure 4. Here, notable differences were observed. For example, the top-scoring inhibitor with the highest differentiation potential had only one nearest neighbor, the fourth-ranked compound (Figure 4a). Equivalent observations were made for inhibitors at rank 3 (Figure 4c) and 4 (Figure 4d). By contrast, the inhibitor at rank 2 (Figure 4b) had a total of 12 nearest structural neighbors with variable differentiation potentials. Similar observations were made for inhibitors at ranks 5 (Figure 4e) and 6 (Figure 4f), having four and six neighbors, respectively. These compounds also displayed low to intermediate differentiation potential. From these compound series, SAR patterns emerged, as discussed in the following.

dx.doi.org/10.1021/jm3014508 | J. Med. Chem. 2012, 55, 11067−11071

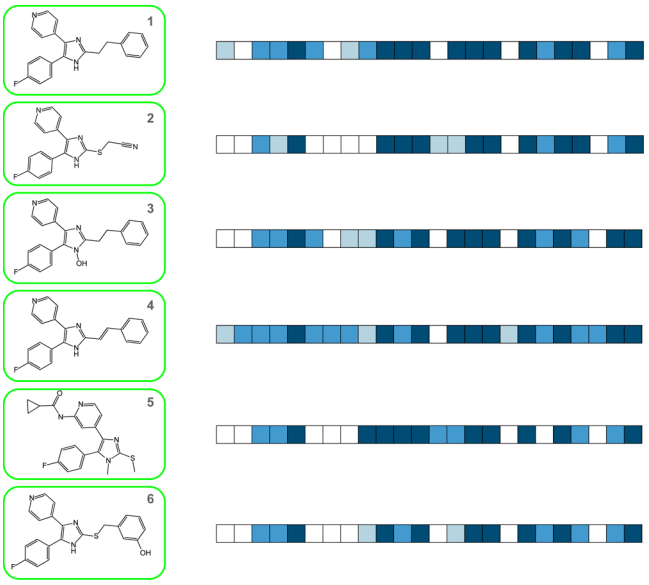

Figure 3. Top-ranked kinase inhibitors. Shown are the six top-ranked compounds with highest differentiation potential (labeled with their ranks) together with their activity profiles (color-coded according to Figure 1). In the activity profile, each bin is assigned to one of the 24 kinases.

SAR Analysis. All tested compounds were initially designed as potential p38α MAP kinase inhibitors. The major novelty of these imidazole-based series is the 2-thio substitution, which greatly reduces their ability to bind to cytochrome P450 (CYP) enzymes by complexing the iron in the active site. This CYP interaction presented a general problem associated with first-generation imidazole-based inhibitors. Kinase profiles of a large set of structurally closely related inhibitors have not yet been described. However, the results reported herein demonstrate how even minor structural modifications of closely related inhibitors can alter the inhibition profile toward kinases other than p38, including representatives of kinase families with rather different functions such as receptor tyrosine kinases.

The computational approach designed for the analysis of the kinase profiling matrix did not take structural information about the kinase ATP binding site into account. Nevertheless, it detected activity differences between compounds that were consistent with structural data of p38−inhibitor interactions. Figure 5 shows an outline of p38 bound to the ATP site-directed pyridinylimidazole inhibitor SB203580,[22] as revealed by the X-ray structure of the complex.[23] A critically important hydrogen bond is formed between the pyridin-4-yl group and the backbone NH of Met109. Another hydrogen bond is formed between Lys53 and N-3 of the imidazole core. In addition, there is a $\pi-\pi$ stacking between Tyr35 and the phenyl ring of the inhibitor. The 4-fluorophenyl ring is accommodated in hydrophobic region I, while hydrophobic region II is not occupied. On the basis of these interaction patterns, structural modifications of imidazole-based inhibitors that led to changes in their differentiation potential according to Figure 4 can be rationalized. For example, the compounds in Figure 4b,c very well reflect the relevance of the $\pi-\pi$ interaction of the S-residues at the R3 position with Tyr35 in p38, as indicated in Figure 5. In Figure 4b, **2** with an acetonitrile group at this position had overall highest differentiation potential, whereas smaller or larger (aromatic) substituents at this position led to a gradual loss of this potential. Phenyl-based substituents such as

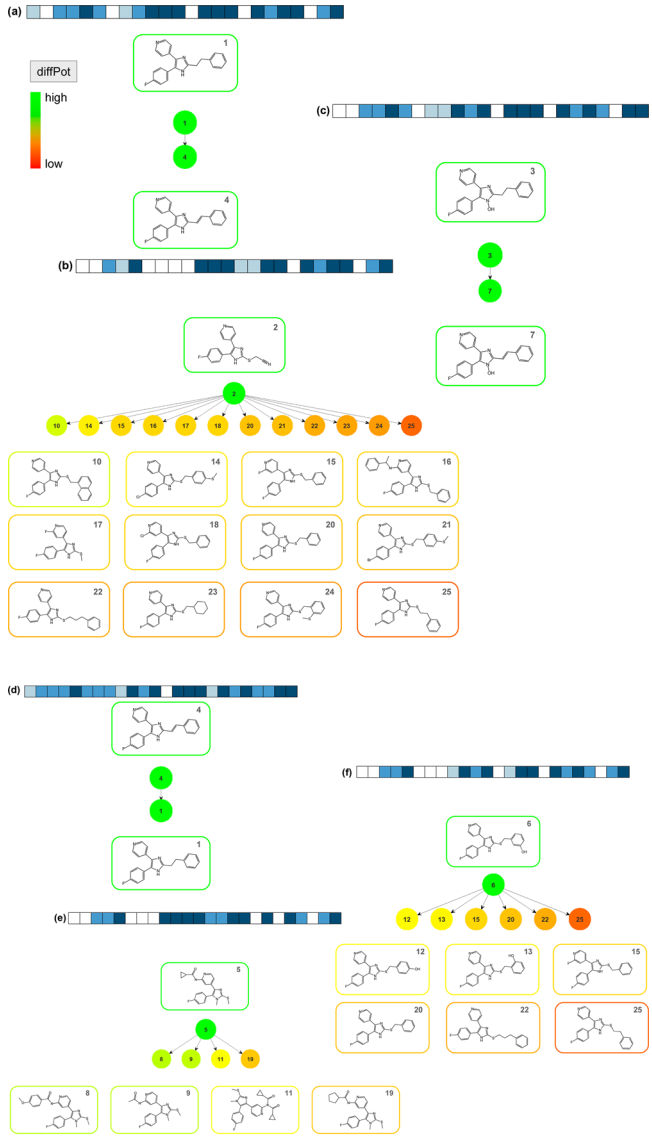

Figure 4. Top-ranked inhibitors and nearest neighbors. In (a) to (f), the six compounds with highest differentiation potential are shown together with their nearest structural neighbors (i.e., all other compounds having at least 80% 2D structural similarity). In the center, each of the six top-ranked compounds is represented as the root node and nearest neighbors form leaves. The nodes are color-coded according to differentiation potential as in Figure 2. The activity profile of the root compound is displayed, and compound structures are drawn proximal to their nodes. Multiple nearest neighbors are arranged according to decreasing differentiation potential from the left to the right.

$\pi-\pi$ interactors were generally more difficult to accommodate than the acetonitrile group because they required a coplanar orientation for best interactions. As illustrated in Figure 4c, loss of R-group flexibility to adopt a favorable geometry for the $\pi-\pi$ interaction also resulted in a penalty and altered the differentiation potential observed for a compound with a conformationally unrestricted phenyl group.

In our kinase panel, JNK3 was most closely related to p38. The only difference in the ATP-binding site of these kinases is the gatekeeper residue, which is Thr in p38 and Met in JNK3. Met is larger but has a flexible side chain and can conformationally adapt. Given the similarity of these kinases,

dx.doi.org/10.1021/jm3014508 | J. Med. Chem. 2012, 55, 11067−11071

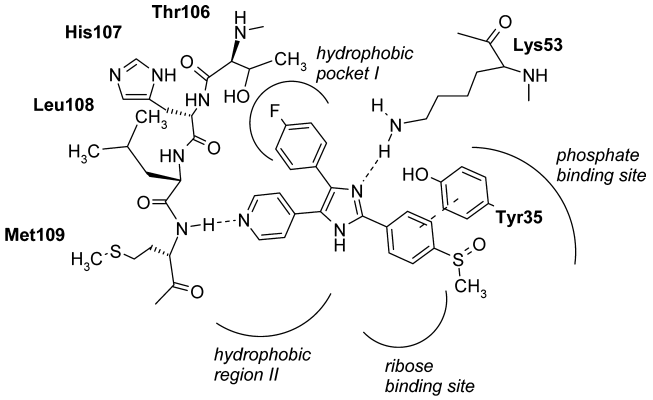

Figure 5. p38–inhibitor complex. Shown is the structure of the ATP binding site in p38 in complex with the pyridinylimidazole inhibitor SB203580.

many compounds inhibited them comparably. However, nearest neighbor analysis also revealed interesting exceptions. For example, **2** with its acetonitrile substituent was highly active against p38 and JNK3. By contrast, **15**, a structural neighbor of **2** with a phenyl group at the corresponding position, retained high activity against p38 but was not active against JNK3. Similarly, **25**, another structural neighbor with an additional methylene group in the linker presenting the phenyl substituent, showed reduced activity against P38 and was also inactive against JNK3. Both of these compounds had overall only low differentiation potential. In the panel, AKT1 was the kinase most distantly related to p38. Accordingly, many of the p38-directed compounds did not inhibit AKT1. However, there were exceptions among compounds with high differentiation potential. For example, **1** and **4** strongly inhibited p38 but also displayed weak activity against AKT1.

Furthermore, very small structural changes between compounds with high differentiation potential preferentially affected certain subsets of kinases. For example, **1** and **4** were only distinguished by the presence of a double bond in the linker between the imidazole core and a phenyl substituent (thus slightly reducing the conformational flexibility of **4**). This minute change led to overall higher activity of **4** against the kinase panel than **1**. In particular, it affected binding to cyclin-dependent kinases, against which **4** was active but **1** only weakly active or inactive. In addition, the presence of a hydrophilic group in this region of the inhibitors, for example, in **6**, led to a complete loss of activity against these kinases. Another interesting example was inhibition of PLK1. Among compounds with significant differentiation potential, only **4**, **7**, and **10** inhibited this kinase; all others were inactive. Compounds **4** and **7** were structurally highly similar, but in **10**, the conformationally restricted phenyl substituent was replaced by an unrestricted naphthalene group. Despite this change, the activity profiles of all three compounds were overall similar and distinct from many others.

Differentiation Potential versus Selectivity. Differentiation potential as assessed herein is related to but distinct from compound selectivity, for which other measures have been introduced in the kinase inhibitor field. These include, among others, the Ambit selectivity score[24] and the thermodynamic partition index.[25] The latter coefficient reflects the partitioning of inhibitor binding across a panel of kinases at thermodynamic equilibrium and should thus be calculated on the basis of equilibrium constants (i.e., K_i or K_d). Hence, it is not applicable to residual activities or other approximate measurements. The Ambit score (AS) is calculated as the fraction of n tested kinases that are inhibited by a compound at a given threshold value of residual activity. Hence, a score of 0 indicates a compound that is inactive at the selected threshold and a score of 1 a compound that is consistently active and nonselective. By contrast, a target-selective compound obtains a score of $1/n$ (close to 0). We have calculated AS values for all compounds for a threshold value of less than 60% residual activity, as reported in Table S2 of the Supporting Information. The mean and standard deviation of the AS distribution are 0.31 and 0.22, respectively. For **1**–**6** with the highest target differentiation potential, scores range from 0.54 and 0.83. Hence, these compounds would not be considered on the basis of simple selectivity scoring. At lower levels of residual activity (e.g., 30%), the scores consistently decrease and equivalent conclusions are drawn. These results reflect the conceptual difference between target differentiation potential and target selectivity of inhibitors. Compounds with differentiation potential are often rich in multitarget SAR information.

CONCLUSIONS

Herein we have reported a compound profiling experiment on a set of cancer-relevant kinases using ATP site-directed imidazole derivatives, combined with a computational study to identify compounds with kinase differentiation potential. Several structurally closely related inhibitors with high differentiation potential were identified, and SAR features were explored on the basis of nearest neighbor analysis. In a number of instances, small structural modifications of closely related compounds led to substantial alterations of their inhibitory profiles, in part involving kinases with different functions. On the basis of these results, the evaluated compound series should merit further consideration in the development of selective kinase inhibitors. Furthermore, the computational approach reported herein is readily applicable to the analysis of other compound profiling experiments and the identification of active small molecules with target differentiation potential.

ASSOCIATED CONTENT

Supporting Information

Table S1 listing complete 484 × 24 kinase profiling matrix and Table S2 listing the distribution of AS values for all compounds. This material is available free of charge via the Internet at http://pubs.acs.org.

AUTHOR INFORMATION

Corresponding Author

*For S.L.: phone, +49-7071-2978788; fax, +49-7071295037; e-mail, Stefan.laufer@uni-tuebingen.de. For J.B.L phone, +49-228-2699-306; fax, +49-228-2699-341; e-mail, bajorath@bit.uni-bonn.de.

Author Contributions

‖The contributions of these two authors should be considered equal.

Notes

The authors declare no competing financial interest.

ACKNOWLEDGMENTS

The authors are grateful to Dagmar Stumpfe for help with data preparation.

■ ABBREVIATIONS USED

AS, Ambit score; ATP, adenosine triphosphate; CV, coefficient of variation; CYP, cytochrome P450; diffPot, differentiation potential; SAR, structure−activity relationship

■ REFERENCES

(1) Rix, U.; Superti-Furga, G. Target Profiling of Small Molecules by Chemical Proteomics. *Nat. Chem. Biol.* **2009**, *5*, 616−624.

(2) Bajorath, J. Computational Analysis of Ligand Relationships within Target Families. *Curr. Opin. Chem. Biol.* **2008**, *12*, 352−358.

(3) Kenakin, T. Functional Selectivity in GPCR Modulator Screening. *Comb. Chem. High Throughput Screening* **2008**, *11*, 337−343.

(4) Allen, J. A.; Roth, B. L. Strategies To Discover Unexpected Targets for Drugs Active at G Protein-Coupled Receptors. *Annu. Rev. Pharmacol. Toxicol.* **2011**, *51*, 117−144.

(5) Goldstein, D. M.; Gray, N. S.; Zarrinkar, P. P. High-Throughput Kinase Profiling as a Platform for Drug Discovery. *Nat. Rev. Drug Discovery* **2008**, *6*, 391−397.

(6) Bi, K.; Lebakken, C. S.; Vogel, K. W. Transformation of in Vitro Tools for Kinase Profiling: Keeping an Eye over the Off-Target Liabilities. *Expert Opin. Drug Discovery* **2011**, *6*, 701−712.

(7) Fabian, M. A.; Biggs, W. H., 3rd; Treiber, D. K.; Atteridge, C. E.; Azimioara, M. D.; Benedetti, M. G.; Carter, T. A.; Ciceri, P.; Edeen, P. T.; Floyd, M.; Ford, J. M.; Galvin, M.; Gerlach, J. L.; Grotzfeld, R. M.; Herrgard, S.; Insko, D. E.; Insko, M. A.; Lai, A. G.; Lélias, J. M.; Mehta, S. A.; Milanov, Z. V.; Velasco, A. M.; Wodicka, L. M.; Patel, H. K.; Zarrinkar, P. P.; Lockhart, D. J. A Small Molecule−Kinase Interaction Map for Clinical Kinase Inhibitors. *Nat. Biotechnol.* **2005**, *23*, 329−336.

(8) Metz, J. T.; Johnson, E. F.; Soni, N. B.; Merta, P. J.; Kifle, L.; Hajduk, P. J. Navigating the Kinome. *Nat. Chem. Biol.* **2011**, *7*, 200−202.

(9) Milletti, F.; Hermann, J. C. Targeted Kinase Selectivity from Kinase Profiling Data. *ACS Med. Chem. Lett.* **2012**, *3*, 383−386.

(10) Martin, E.; Mukherjee, P. Kinase-Kernel Models: Accurate in Silico Screening of 4 Million Compounds across the Entire Human Kinome. *J. Chem. Inf. Model.* **2012**, *52*, 156−170.

(11) Niijima, S.; Shiraishi, A.; Okuno, Y. Dissecting Kinase Profile Data To Predict Activity and Understand Cross-Reactivity of Kinase Inhibitors. *J. Chem. Inf. Model.* **2012**, *52*, 901−912.

(12) Laufer, S. A.; Wagner, G. K. From Imidazoles to Pyrimidines: New Inhibitors of Cytokine Release. *J. Med. Chem.* **2002**, *45*, 2733−2740.

(13) Laufer, S. A.; Kotschenreuther, D.; Wagner, G. K. Ones, Thiones and *N*-Oxides: An Exercise in Imidazole Chemistry. *Angew. Chem., Int. Ed.* **2002**, *41*, 2290−2293.

(14) Laufer, S. A.; Striegel, H.-G.; Wagner, G. K. Imidazole Inhibitors of Cytokine Release: Probing Substituents in the 2 Position. *J. Med. Chem.* **2002**, *45*, 4695−4705.

(15) Laufer, S. A.; Kotschenreuther, D. A.; Wagner, G. K.; Albrecht, W. Novel Substituted Pyridinyl Imidazoles as Potent Anti-Cytokine Agents with Low Cytochrome P450 Activity. *J. Med. Chem.* **2003**, *46*, 3230−3244.

(16) Laufer, S. A.; Kotschenreuther, D. A.; Wagner, G. K. Identification of Regioisomers in a Series of N-Substituted Pyridin-4-yl-imidazole Derivatives by Regiospecific Synthesis, GC/MS and ^{1}H-NMR. *J. Org. Chem.* **2003**, *68*, 4527−4530.

(17) Laufer, S. A.; Striegel, H.-G.; Zimmermann, W.; Ruff, K. J. Tetrasubstituted Imidazole Inhibitors of Cytokine Release: Probing Substituents in the N-1 Position. *J. Med. Chem.* **2004**, *47*, 6311−6325.

(18) ProQinase Free Choice Biochemical Kinase Assays. http://www.proqinase.com/ (accessed September 3, 2012).

(19) Dimova, D.; Bajorath, J. Computational Chemical Biology: Identification of Small Molecular Probes that Discriminate between Members of Target Protein Families. *Chem. Biol. Drug Des.* **2012**, *79*, 369−375.

(20) Willett, P.; Barnard, J. M.; Downs, G. M. Chemical Similarity Searching. *J. Chem. Inf. Comput. Sci.* **1998**, *38*, 983−996.

(21) *MACCS Structural Keys*; Symyx Software: San Ramon, CA, U.S., 2005.

(22) Wagner, G.; Laufer, S. Small Molecular Anti-Cykotine Agents. *Med. Res. Rev.* **2006**, *26*, 1−62.

(23) Tong, L.; Pav, S.; White, D. M.; Rogers, S.; Crane, K. M.; Cywin, C. L.; Brown, M. L.; Pargellis, C. A. A Highly Specific Inhibitor of Human p38 MAP Kinase Binds in the ATP Pocket. *Nat. Struct. Biol.* **1997**, *4*, 311−316.

(24) Karaman, M. W.; Herrgard, S.; Treiber, D. K.; Gallant, P.; Atteridge, C. E.; Campbell, B. T.; Chan, K. W.; Ciceri, P.; Davis, M. I.; Edeen, P. T.; Faraoni, R.; Floyd, M.; Hunt, J. P.; Lockhart, D. J.; Milanov, Z. V.; Morrison, M. J.; Pallares, G.; Patel, H. K.; Pritchard, S.; Wodicka, L. M.; Zarrinkar, P. P. A Quantitative Analysis of Kinase Inhibitor Selectivity. *Nat. Biotechnol.* **2008**, *26*, 127−132.

(25) Cheng, A. C.; John Eksterowicz, J.; Geuns-Meyer, S.; Sun, Y. Analysis of Kinase Inhibitor Selectivity Using a Thermodynamics-Based Partition Index. *J. Med. Chem.* **2010**, *53*, 4502−4510.